scientific reports

OPEN

Expanded CD16+CD56+Granzyme B+ NK like CD8+ T cells an off target effect of bruton's tyrosine kinase inhibitors in Waldenström macroglobulinemia

Priyanka Hastak[1,6]✉, Chansavath Phetsouphanh[1,6], Zong-Hong Zhang[1], Rowena A. Bull[1,3], Lok Bahadur Shrestha[1,3], Vera Klemm[4], Raymond Louie[5], Fabio Luciani[3], C. Mee Ling Munier[1], Alexandra Carey Hoppé[1], Elizabeth Keoshkerian[3], Brendan Beaton[2], Katherine Rankin[2], Alexander Wong[2], Judith Trotman[2], Anthony D. Kelleher[1] & Sarah C. Sasson[1]

Bruton's tyrosine kinase inhibitors (BTKi), widely used in Waldenström macroglobulinemia (WM), are known to impair B cell function, but their broader immunological effects remain unclear. We investigated the T cell compartment in patients with WM receiving BTKi, including those who underwent a supervised treatment pause before a third COVID-19 mRNA vaccine dose, as well as treatment naïve controls. Using flow cytometry, antigen-specific T cell assays, and single-cell RNA sequencing, we found that BTKi-treated patients exhibited a reduction in naïve T cells, enrichment of terminal effector CD8+ T$_{emra}$ cells, and lower PD-1 expression. Despite poor vaccine-induced RBD-specific memory B cells, CD4+ and CD8+ T cell responses to SARS-CoV-2 remained detectable, with enhanced CD8+ responses to the omicron variant in BTKi-treated individuals. Single-cell transcriptomics revealed an expansion of CD16+ CD56+ Granzyme B+ NK-like CD8+ T cells in BTKi-treated patients, which further increased following BTKi interruption. These cells expressed a potent cytotoxic and NK-like transcriptional phenotype. Our findings identify a novel off-target effect of BTKi therapy: expansion of cytotoxic NK-like CD8+ T cells, with implications for immune monitoring and vaccine responsiveness in BTKi-treated patients.

Bruton's tyrosine kinase (BTK) plays a pivotal role in regulating B cell development and function[1]. Individuals with X-linked agammaglobulinemia (XLA) harbour an in-born error in the *BTK* gene, resulting in a primary immunodeficiency characterised by a lack of both mature B cells and antibodies due to impaired B cell maturation. Leveraging the observed impact that XLA has on B cells, immunotherapy with BTK inhibitors (BTKi) are used for B cell depletion in the setting of B cell lymphomas including Waldenström Macroglobulinemia[2].

Waldenström macroglobulinemia (WM) is a rare subtype of non-Hodgkin's B cell lymphoma characterised by IgM immunoglobulin gammopathy and bone marrow infiltration. This malignancy demonstrates clinical heterogeneity ranging from asymptomatic disease to critical hyperviscosity syndromes. In people with WM, the most commonly prescribed BTKi globally is the orally administered ibrutinib which improves progression-free survival[4].

There is some evidence to suggest BTKi may have off-target effects resulting from inhibition of other kinases. Notably, BTKi affects epidermal growth factor kinase, tyrosine kinase SRC linked to B cell activation and Tec kinase, and IL-2 kinase (ITK) involved in T cell signalling, polarization and migration[5]. BTKi, particularly in the form of ibrutinib, has been widely studied in chronic lymphoid leukemia (CLL), where a significant reduction in circulating T cells was reported after 24 weeks of therapy[6]. After 8 weeks of treatment, there was a decrease in

[1]The Kirby Institute, UNSW, Sydney, NSW, Australia. [2]Haematology Department, Concord Repatriation General Hospital, Sydney, NSW, Australia. [3]School of Biomedical Sciences, UNSW, Sydney, NSW, Australia. [4]Clinical Trials Unit, Macquarie University, Sydney, NSW, Australia. [5]School of Computer Science and Engineering, UNSW, Sydney, NSW, Australia. [6]Priyanka Hastak and Chansavath Phetsouphanh: Equal first authors ✉email: phastak@kirby.unsw.edu.au

chronic CD8^{+} T cell activation (low CD38^{+} and HLA-DR^{+}), pseudo-exhaustion (low PD-1^{+} and CTLA4^{+}), and proliferation[7,8]. Ibrutinib has also been associated with an increase in Th1 cells and reduction in Th2 cells after 8–12 months. This suggests ibrutinib leads to perturbations in T cell homeostasis in CLL[9]. However, the exact mechanisms underlying the off-target effects of BTKi on T cells including in other conditions such as WM have not been well-elucidated[7].

Our group and others have previously demonstrated that B-cell depletion therapies, including BTKi had profound, deleterious effects on vaccine seroconversion to the first two doses of COVID-19 vaccine[10–12]. These deficits included reduced anti-Spike IgG levels and live virus neutralization. We additionally studied the effect of a medically supervised, patient-initiated BTKi treatment interruption on vaccine seroconversion to the third dose of BTN162b2 COVID-19 vaccine. A supervised pause in BTKi treatment led to a rise in anti-spike IgG and neutralization response[13], suggesting that interrupting the BTKi treatment may be a viable strategy to maximise response to vaccination. However, to progress this field, more information is needed about the off-target, and specifically T cell response to BTKi treatment and interruption. This is particularly relevant given that a number of BTKi are currently in ongoing Phase II trials in multiple sclerosis (MS), a disease where both B and T cells play pathogenic roles[14].

Here we compared the response to the third dose of the mRNA COVID-19 vaccine in the following groups (1) people with WM on continuous BTKi therapy (2) those that underwent a supervised BTKi treatment interruption[13] and (3) patients with untreated WM. For the first time, we investigated the antigen-specific B cell and T cell responses in people with WM on BTKi continuous and interrupted treatment. We further investigated the transcriptome dynamics within these cohorts post third COVID-19 vaccine dose using single-cell RNA sequencing. We aimed to determine if there was a compensatory enhancement of antigen-specific T cell responses, given the absence of B cells, in BTKi-treated patients receiving 3rd dose of COVID-19 vaccines, using a single cell transcriptomic approach.

Methods

Participants and sample collection

Peripheral blood mononuclear cells (PBMCs) were isolated and cryopreserved within 2 weeks of a 3rd dose of mRNA COVID-19 (Moderna Spikevax/BNT162b2) vaccine (see Supplementary Fig. 1). Our groups of participants were: (1) Healthy volunteers ($N=10$) (2) Patients with WM ($N=9$) on continuous BTKi treatment; (3) Patients with WM who underwent a BTKi treatment pause prior to the third vaccine dose ($N=9$); (4) Treatment naïve patients with WM ($N=5$); (5) The Group 3 participants who underwent BTKi treatment pause self-interrupted their BTKi therapy for 3–4 days prior to the third vaccine dose and resumed therapy at a median of 24 days (range 18–31 days) after the third dose (D3) of the vaccine, depending on their willingness and tolerance for treatment interruption. These patients were closely monitored by specialist physicians in weekly clinical reviews.

This study has the appropriate approval from the ethics committee, Sydney Local Health District Human Research Ethics (2021/ETH00840 and 2021/ETH00180) for experiments.

Informed consent was obtained from all the subjects and/or their legal guidance. Patient characteristics are provided in Supplementary Table 1. All the methods were carried out in accordance with relevant guidelines and regulations.

Ex vivo phenotyping and activation-induced T cell marker assay

Cryopreserved PBMCs were thawed using RPMI (L-glut) medium (ThermoFisher Scientific, USA) supplemented with penicillin/streptomycin (Sigma-Aldrich, USA) and 10% heat inactivated Fetal Calf Serum (ThermoFisher Scientific, USA), and subsequently stained with live/dead dye Near InfraRed and antibodies binding to extracellular markers. The extracellular panel included:, CXCR5 (MU5UBEE), CD38 (HIT2) (ThermoFisher Scientific, USA); CD3 (UCHT1), CD8 (HIL-72021), PD-1 (EH12.1), TIM-3 (TD3), CD27 (L128), CD45RA (HI100), IgD (IA6-2), CD25 (2A3), and CD19 (HIB19) (Biolegend, USA); CD4 (OKT4), CD127 (A019D5), HLA-DR (L234), GRP56 (191B8), CCR7 (G043H7) and CD57 (QA17A04) (BD Biosciences, USA). Perm Buffer II (BD Pharmingen) was used for intracellular staining of granzyme B (GB11, BD Biosciences). FACS staining of 48 h activated PBMCs was performed as previously described[15], but with the addition of CD137 (4B4-1) to the cultures at 24 h. Final concentration of 10 µg/mL of SARS-CoV-2 peptide pools (Genscript) were used, 1 µg/mL of Fluarix tetra (Influenza vaccine-GSK) was used as a control antigen and SEB (Staphylococcus enterotoxin B) was used as a positive control (Thermo Fisher Scientific). In vitro activation assay monoclonal antibody (mAb) panel included: CD3 (UCHT1), CD4 (RPA-T4), CD8 (RPA-T8), CD39 (A1), CD69 (FN50) all from Biolegend, and CD25 (2A3), CD134 (L106), CD137 (4-1BB) from BD Biosciences. Samples were acquired on an Cytek Aurora (Cytek Biosciences, USA) using the Spectroflo software and single-color reference controls were run for unmixing. Prior to each run, all samples were fixed in 0.5% paraformaldehyde/PBS (Sigma-Aldrich, USA). Data analysis was performed using Spectroflo version 3.0 (Cytek) (link: https://cytekbio.com/pages/spectro-flo) and FlowJo version 10.7. 1 (BD Biosciences)[16].

Cell trace Violet (CTV) proliferation assays

PBMCs were resuspended at a concentration of $\sim 10 \times 10^6$/ml in PBS and incubated with Cell Trace Violet (CTV) dye (Thermofisher) at 5µM for 20 min at RT, according to the manufacturer's directions. Cells were washed once with 5x volume of IMDM/10% heat inactivated human AB serum (Thermofisher) and resuspended for cultures of 300,000 PBMC in 200 µl/well of a 96-well plate and incubated for 7 days in a 5% CO_2 incubator. Different wells contained different antigens. All experiments also included: (i) culture medium only negative control well; (ii) SEB as a positive control well and (iii) SARS-CoV-2 peptide pool[16]. PBMC from the respective cultures were stained with CD3-PerCP-Cy5.5, CD4-AF700, CD8-BV650 and CD25-APC, and analysed on a 5-laser Cytek

Aurora[17] and antigen-specific CD4^{+} T cells gated as CD3^{+}CD4^{+}CD25^{high}CTV^{dim} or CD3^{+}CD8^{+}CD25^{high}CTV^{dim} as previously described[18]. Cultures were classified as positive for antigen-specific CD4^{+} T cells if the CD25^{high}CTV^{dim} % of CD4^{+} CD3^{+} T cells was ≥ 1%.

Staining SARS-CoV-2 receptor binding domain (RBD)- specific memory B cells

SARS-CoV-2-specific memory B cells were measured using our previously published flow cytometric tetramer assay[19]. In brief, biotinylated Receptor Binding Domain (RBD) was incubated with Streptavidin- PE probes at 4°C. Cryopreserved PBMCs were thawed in a 37°C water bath and washed with RPMI and 10% FCS media (Sigma). A maximum of 1×10^7 cells were stained using Fixable Viability Stain 700 (FVS700) (BD Biosciences) and washed with FACs wash buffer (BD Biosciences). Followed by incubation with 5 μl of Human Fc block (BD) for 2×10^6 cells at room temperature for 10 min. All next steps were conducted on ice or at 4°C. Cells were stained for 30 min with 50 μl stain buffer and 5 μl each of CD21-BV421, IgD-BV510, CD10-BV605, CD19-BV711, CD20-APC H7, IgG-BV786, CD27-PE-CF596, CD38-PE-Cy7, HLA-DR-BB515 antibodies. The cells were washed and sorted on the BD FACSAria III sorter. FlowJo version 10.7.1 (TreeStar) was used to analyse the data.

Sample staining, tagging, and loading on cartridge capture system for single cell RNA sequencing

Cryopreserved PBMCs from all participants were processed, stained, and tagged as described previously (BD Rhapsody™ Single-Cell Analysis System Instrument User Guide[20]. Briefly, PBMCs were thawed in 37 C water bath and washed using RPMI ([+]L-glutamine) medium (ThermoFisher Scientific) and heat inactivated 10% FCS (ThermoFisher Scientific). ~1 million cells were collected from the 9 participants (N = 3 each for treatment naïve, BTKi and BTKi paused) and index tag (BD Rhapsody) was added to each. We excluded healthy controls from this experiment. Following protocol as described previously, these samples were pooled together and washed with 1X DPBS (Life Technologies). The pooled cells were stained using 1 μl live-dead NIR (ThermoFisher Scientific) dye and incubated in the dark for 30 min. Extracellular staining was performed using 10 μl each of BD Brilliant Dye Buffer, CD45RO-BV510 (BD Biosciences), CD3-PECF594 (BD Biosciences) and CD20-BV605 (BD Biosciences). The BD FACSAria III Cell Sorter was used for first sorting live/dead and CD45RO^{+} cells followed by gating for T cells (CD3) and B cells (CD20) pooled together.

~1 million of these sorted cells were stained with the AbSeq Immune Discovery Panel cocktail as previously described (BD Rhapsody™ Single-Cell Analysis System Instrument User Guide (Doc ID: 214062). Single-cell capture of 18,500 cells on single cell cartridge with the BD Rhapsody single-cell analysis system was conducted following the BD Rhapsody protocols. Briefly, the steps involved staining, loading, lysis, retrieving capture beads and exonuclease treatment.

Library preparation and sequencing

The mRNA whole transcriptome analysis (WTA), AbSeq and sample tag library preparation followed by quantification and library quality check was set up using the BD Rhapsody System protocol (BD Rhapsody™ Single-Cell Analysis System Instrument User Guide (Doc ID: 214062). Single-cell gene matrices corresponding to Unique Molecular Identifier (UMI) counts from BD Rhapsody Whole Transcriptome Analysis (WTA) assays were produced using the BD Rhapsody (Seven Bridges) WTA analysis pipeline, which included read quality filtering, alignment to the GRCh38 reference genome, UMI counting and error correction. Paired-protein matrices for each cell were also obtained from BD AbSeq Ab-Oligos (antibody-oligonucleotides) experiments and processed using the same Rhapsody pipeline with alignment to an AbSeq reference (BD AbSeq Immune Discovery Panel).

Cell quality control was performed on all samples, which involved removing cells with low/high total mRNA counts (1000/6363 ~ 9635), number of unique genes (400/1883 ~ 2265) and mitochondrial content (0.01 ~ 0.1/0.3 ~ 0.4) and removing all doublets. After quality control, gene expression matrices were normalized using Scran[21], while protein expression matrices were normalized using the centred-log-ratio (CLR) normalization from the Seurat package (v4.1.1).

Normalized gene expression matrices were integrated using Seurat (v4.1.1)[22]. The functions 'FindIntegrationAnchors' and 'IntegrateData' were used to identify cross-dataset pairs of cells that were in a matched biological state ('anchor'), then these anchors were used to integrate multiple datasets. Dimensionality reduction was performed on the integrated dataset by the RunPCA function using top 3000 highly variable genes or all genes if the total number of gene is less than 3000. The variable genes were obtained by the FindVariableFeatures function (npcs = 30). Clustering was then performed on the integrated data set by the FindCluster function in Seurat (v4.1.1)[22], which identified clusters of cells using a shared nearest neighbour (SNN) modularity optimization-based clustering algorithm.

Resolution parameters ranging from of 0.1 to 1.4 were explored to identify the optimal number of clusters, with 0.4 being selected for the clustering in this study. For each sample, Differentiation Gene Expression analysis (DGE) using MAST and Differentiation Protein Expression analysis (DPE) using Wilcoxon Rank sum test were first performed on each cluster. Marker gene and proteins were chosen if they were statistically significant ($p < 0.1$) and had a high fold change (average log2FC > 0.014) in the majority of samples. Uniform Manifold Approximation and Projection (UMAP) was then used for dimensionality reduction to visualize the clustering results with nearest neighbour as 30 and mid_dist as 0.01. The dot plots were generated using ggplot2, with the gene expression averages value obtained over all samples.

Inter-condition differentiation gene expression (DGE) and differentiation protein expression (DPE) analysis were performed using the edgeR (v.3.40.0) wrapper run_de function in the Libra R package[23] with the likelihood-ratio (LRT) and pseudobulk option, with patients under each condition serving as replicates. The inter-condition

comparisons (DGE and DPE) include each pair of conditions defined above and the combination of those conditions, BTKi and BTKi pause group vs. treatment naive.

To determine significant pathways, gene set enrichment analysis (GSEA) was performed, which is a computational method that determines whether a priori defined gene sets show statistically significant, concordant differences between two biological states. Gene sets used in GSEA were the canonical hallmark gene sets obtained from the MSigDB database[24]. GSEA was performed by the fgsea function from the fgsea R package[25] with default parameters, based on DGE results ranked by the fold-change between biological states.

Statistical analysis

All column graphs are presented as medians with inter-quartile ranges. For multiple comparisons we used one way ANOVA employing Prism 10 (GraphicPad, La Jolla, CA, USA) software. For non-parametric comparisons between two groups, the Mann-Whitney U test (two-sided) was used. For multiple group comparisons, the Kruskal-Wallis test was performed, followed by pairwise Mann-Whitney U tests. Significance set at $p < 0.05$. Medians were calculated with 95% CI. For single cell RNA sequencing data to determine the significant difference in the proportion of cells across treatment groups, we utilized the two-proportion Z-test.

Results

Low B cell frequencies and high CD8⁺ T cell frequencies evident in WM patients on BTKi treatment compared to healthy controls

Ex-vivo phenotyping by spectral flow cytometry was conducted in BTKi treated, BTKi paused, and treatment patients and healthy controls. Data was analysed using pair-wise Mann-Whitney U test (two-sided) to compare median values. B cell frequencies were significantly lower in BTKi treated patients (median = 1.05%), averaging 3.77-fold less than in healthy controls (median 3.85%, $p = 0.012$) (Supplementary Fig. 2A) but there was no significant difference compared to treatment naïve patients (median = 0.36%, $p = 0.797$) and healthy controls and treatment naïve patients ($p = 0.095$) (Supplementary Fig. 2A). Pausing BTKi treatment before the 3rd dose did not significantly increase the B cell proportion (median = 0.23% for BTKi vs. 1.05% for BTKi pause, $p = 0.904$) (Supplementary Fig. 2B).

Lower frequencies of CD4⁺ T cells were observed in BTKi treated patients (median = 55.3%) compared to healthy controls but this did not reach significance (median = 67.3%, $p = 0.058$) (Fig. 1A). There was no difference in the proportion of CD4⁺ T cells between BTKi treated patients and treatment-naive (median = 52.5%, $p = 0.770$) patients (Fig. 1A). Notably, BTKi treated patients exhibited significantly higher frequencies of CD8⁺ T cells (median = 36.4%) compared to healthy controls (median = 21.2%, $p = 0.038$) in contrast to treatment naïve patients (median = 34.2%, $p = 0.898$) (Fig. 1B). Interestingly BTKi treated patients had a significantly lower CD4:CD8 proportions (median = 1.88%) compared to healthy controls (median = 3.72%, $p = 0.042$) (Fig. 1C).

Pausing BTKi treatment before the 3rd COVID-19 vaccine dose was associated with reduced CD4⁺ T cell proportion (median = 57.4% for BTKi vs. 42.6% for BTKi pause, $p = 0.103$) (Supplementary Fig. 3A) and the CD4⁺:CD8⁺ ratio population but this did not reach statistical significance (median = 2.4% vs. 0.7, $p = 0.285$) (Supplementary Fig. 3C). For CD8 T⁺ cell proportions there was a slight increase after the interruption, but this did not reach statistical significance (median = 26.8% for BTKi vs. 43.8% for BTKi pause, $p = 0.218$) (Supplementary Fig. 3B). These non-significant trends in BTKi paused patients may be as a result of the relatively brief BTKi treatment interruption.

Reduced naïve T cell subsets, increased T_em and exhaustion marker expression on CD4⁺ and CD8⁺ T cells in BTKi treated WM patients compared to healthy controls

BTKi-treated patients displayed a non-significant trend toward lower frequencies of naïve CD4⁺ T cells (median = 23.5%) compared to healthy controls (median = 42%, $p = 0.297$) (Fig. 2A, see Supplementary Fig. 4
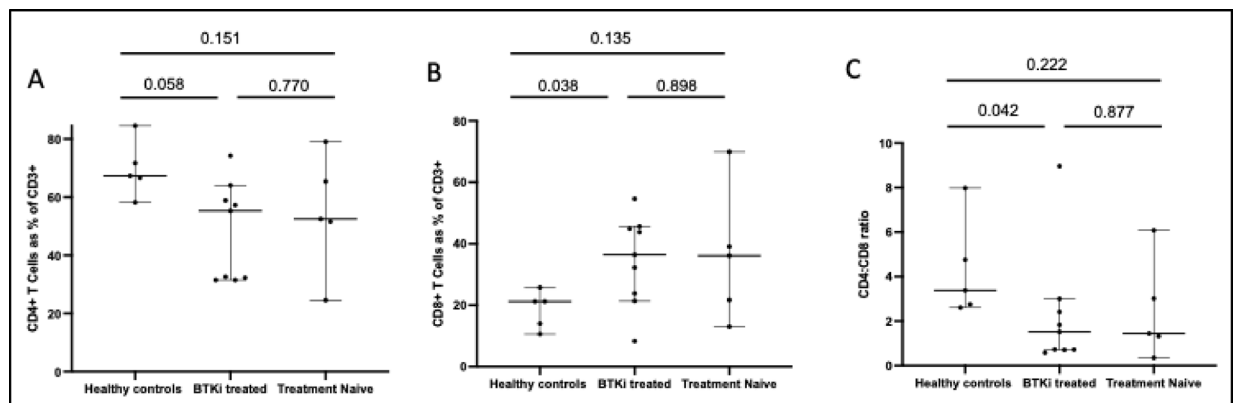

Fig. 1. Proportion of CD4⁺ (**A**) and CD8⁺ (**B**) T cells and CD4⁺:CD8⁺ ratios (**C**) following dose 3 (D3) of mRNA COVID-19 vaccination in healthy controls, BTKi treated, treatment naïve patients at D3. Median percentage are shown with interquartile range. Mann Whitney U test was conducted for pairwise comparison and Kruskal–Wallis tests to evaluate all groups simultaneously. p values < 0.05 were considered significant.
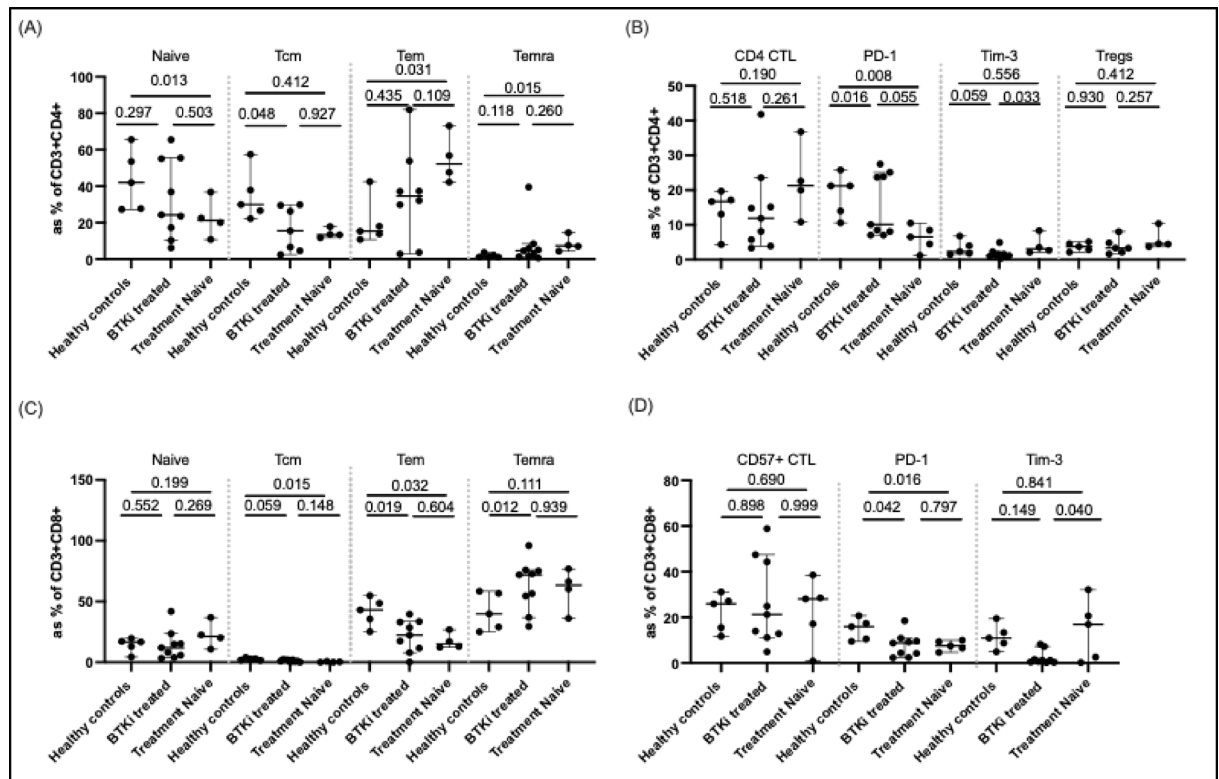
Fig. 2. T cell profiling following dose 3 (D3) of mRNA COVID-19 vaccination in patients with Waldenström Macroglobulinaemia (WM) who were treatment naïve or treated with Bruton's tyrosine kinase inhibitors (BTKi) in addition to healthy controls. T_{cm}= central memory T cells, T_{em}= effector memory T cells, T_{emra}= terminally differentiated effector memory T cells, CTL = cytotoxic T cells. (**A**) CD4$^+$ T cells belonging to naïve, T_{cm}, T_{em}, T_{emra} subsets across 3 patient groups. (**B**) CD4 T cells belonging to CTL, PD-1, TIM-3 and T_{reg} subsets across 3 patient groups. (**C**) CD8$^+$ T cells belonging to naïve, T_{cm}, T_{em}, T_{emra} subsets across 3 patient groups. (**D**) CD4 T cells belonging to CTL, PD-1, TIM-3 and T_{reg} subsets across 3 patient groups. Median percentage are shown with interquartile range. Mann Whitney U test was conducted for pairwise comparison and Kruskal–Wallis tests to evaluate all groups simultaneously. p values < 0.05 were considered significant.

for gating strategy). A reduction in effector memory (T_{em}) and terminally differentiated effector memory (T_{emra}) CD4$^+$ T cells was also observed in BTKi-treated patients (medians = 34.6% and 4.6%) compared to treatment-naïve patients (medians = 52.2% and 7.6%), although these differences did not reach significance (p = 0.109 and p = 0.260). Notably, treatment-naïve patients had significantly higher frequencies of CD4$^+$ T_{emra} cells compared to healthy controls (median = 0%, p = 0.015), suggesting a WM disease-driven effect (see Fig. 2A). Further details on the medians, mean and percentile for CD4$^+$ and CD8$^+$ T cells as well as B cells provided in Supplementary Table 2.

PD-1 expression on CD4$^+$ T cells was significantly lower in BTKi-treated patients (median = 11.9%) compared to healthy controls (median = 16.7%, p = 0.016) (Fig. 2B), indicating reduced expression of this exhaustion marker.

A significant reduction in naïve CD8$^+$ T cells was observed in treatment-naïve patients (median = 21.3%) compared to healthy controls (p = 0.013), while no significant differences were observed between BTKi-treated patients and the other groups (p = 0.552 comparing with healthy controls and p = 0.269 comparing with treatment naïve) (Fig. 2C). CD8$^+$ T_{em} cell frequencies did not differ significantly across groups (Fig. 2C). In contrast, T_{emra} CD8$^+$ T cells were significantly higher in BTKi-treated patients (median = 72.6%) compared to healthy controls (median = 39.8%, p = 0.012) (Fig. 2C).

PD-1 expression on CD8$^+$ T cells did not significantly reduce in BTKi-treated patients (median = 9.63%) compared to healthy controls (median = 16.9%, p = 0.042) (Fig. 2D). Additionally, treatment-naïve patients had even lower CD8$^+$ PD-1 expression compared to healthy controls (median = 6.22%, p = 0.016 vs. healthy controls) (Fig. 2D).

Antigen-specific T cell responses detectable but no difference in T cell proliferation in WM patients

Activation-induced marker expression was used to assess T cell recall memory by identifying SARS-CoV-2 spike-specific T cells following 3rd dose of vaccination in healthy controls, BTKi treated, treatment naïve and BTKi paused patient groups. Co-expression of CD25$^+$ and CD134$^+$ on CD4$^+$ T cells was measured 48 h after

stimulation with SARS-CoV-2 spike peptides, using separate pools representing the ancestral and Omicron (BA.1) strains.

The co-expression of CD25^{+} and OX40^{+} was used to identify antigen-specific CD4^{+} T cells. Ancestral spike-specific CD4^{+} T cell response was similar in BTKi treated groups (median = 0.56%) compared to healthy controls (median = 0.66%, $p = 0.962$) and treatment naïve patients (median = 0.64%, $p = 0.953$) or healthy controls compared to treatment naïve ($p = 0.999$) (see Fig. 3A). CD4^{+} T cell responses to the Omicron peptide pool were on average 5-fold lower than responses to the ancestral strain across the patient groups (see Fig. 3A and B). No significant difference was observed for Omicron CD4^{+} T cell responses between the patient groups. (Fig. 3B). Pausing BTKi treatment before dose 3 of the vaccine did not affect the CD4^{+} T cell responses to both ancestral (median = 0.73% for BTKi vs. 0.56% for BTKi pause; $p = 0.904$, Supplementary Fig. 5A) and Omicron viral strains (median = 0.46% for BTKi vs. 0.35% for BTKi pause; $p = 0.999$, Supplementary Fig. 5B).

The co-expression of CD69^{+} and CD137^{+} was used to identify antigen-specific CD8^{+} T cells. Like ancestral spike-specific CD4^{+} T cell responses, CD8^{+} responses were similar across the treatment groups (see Fig. 3C). CD8^{+} T cell responses to the Omicron peptide pool were on average 7.4-fold lower than responses to the ancestral strain across all patient groups (see Fig. 2C and D). Notably, CD8^{+} memory T cell responses to Omicron were significantly higher in BTKi-treated patients (median = 0.35%) compared to treatment-naive patients (median = 0, $p = 0.005$, Fig. 3D) and healthy controls (median = 0.18%) versus treatment naïve ($p = 0.020$). Pausing BTKi treatment did not affect CD8^{+} T cell responses to ancestral (median = 1.41% for BTKi vs. 0.82% for BTKi pause; $p = 0.722$, see Supplementary Fig. 5C) or Omicron strains (median = 0.25% for BTKi vs. 0.38% for BTKi pause; $p = 0.730$, see Supplementary Fig. 5D). When multiple comparisons were corrected for, there was no significant difference in CD4^{+} and CD8^{+} T cell responses against both omicron and ancestral strains across the patient groups (not shown in figures).

T cell proliferation utilizing Cell Trace Violet dye was measured at day 5 following stimulation with spike peptide pools in treatment naïve, BTKi treated, BTKi paused patients, and healthy controls (see Supplementary Fig. 6A-F). There was no difference in the CD4^{+} and CD8^{+} T cell responses against ancestral or omicron variants.

Decreased RBD-specific memory B cells in BTKi treated WM patients

B cell populations were examined by flow cytometry at following 3rd dose of vaccination for treatment naïve versus grouped BTKi (BTKi treated and paused) patients to determine the treatment effect. Pairwise comparison conducted using two sided Mann Whitney U test ($p < 0.05$). Lymphocytes were gated on CD19^{+}CD20^{+}CD10^{−} and then subsequently gated based on CD27^{+}IgD^{+} and RBD[+](Fig. 4A). A significant decrease in RBD^{+} B
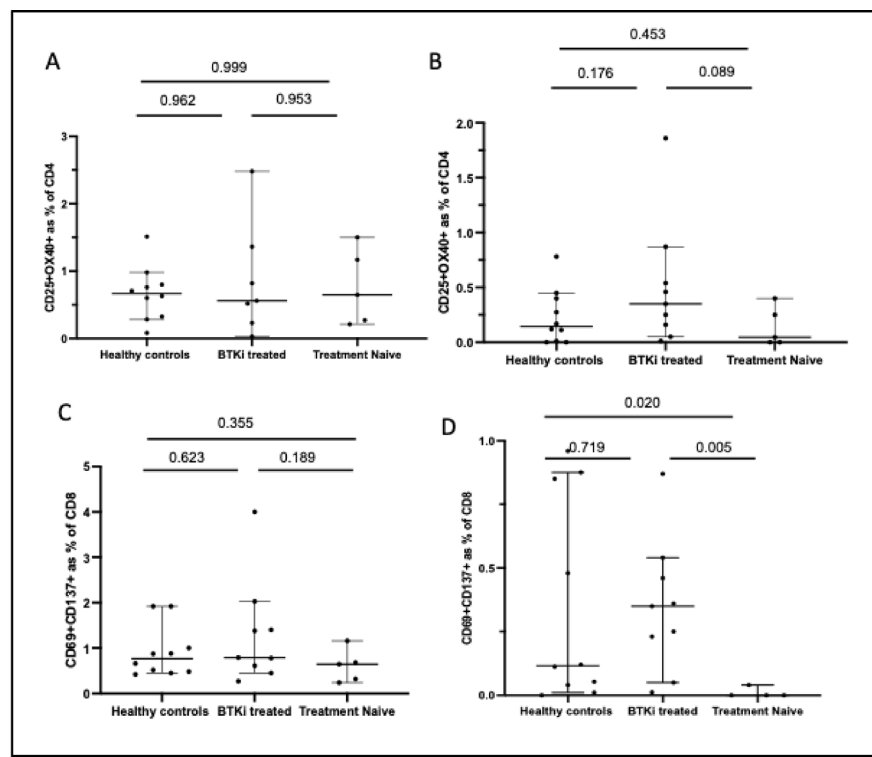

Fig. 3. Detectable antigen specific T cell responses following dose 3 (D3) of mRNA COVID-19 vaccination in healthy controls, BTKi treated and treatment naïve patients. CD4^{+} memory recall responses across these three treatment groups for (**A**) ancestral strain, (**B**) omicron strain. CD8^{+} memory recall responses across three treatment groups for (**C**) ancestral, (**D**) Omicron strain. Median percentage are shown with interquartile range. Mann Whitney U test was conducted for pairwise comparison and Kruskal–Wallis tests to evaluate all groups simultaneously. p values < 0.05 were considered significant.
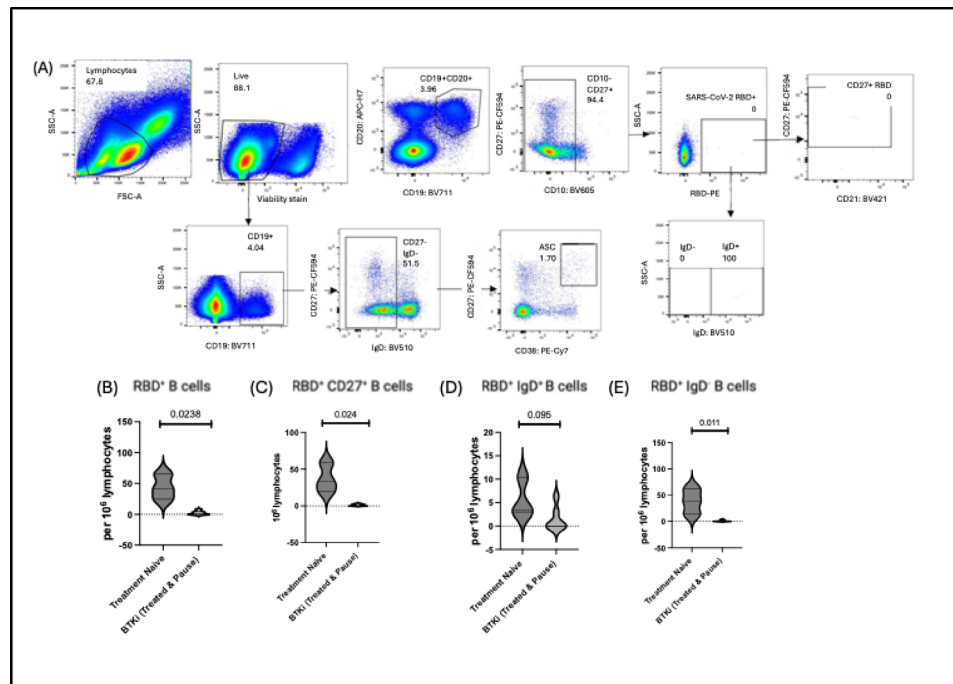
Fig. 4. B cell responses following dose 3 (D3) of mRNA COVID-19 vaccination BTKi treated, treatment naïve and BTKi paused patients. B cells were gated on CD19$^+$CD20$^+$CD10$^-$ and then subsequently gated based on CD27$^+$IgD$^+$ and RBD$^+$ (**A**) Representative flow cytometry plots of live B cells, RBD specific memory and naïve B cells, antibody secreting cells (ASCs). (**B**) RBD$^+$ B cells differed significantly across all 3 treatment groups. (**C**) Naïve B cells did not differ across the 3 treatment groups. (**D**) memory RBD$^+$ B cells were not significantly different across all 3 treatment groups. (**E**) CD19$^+$ CD20$^+$ CD10$^-$ C27$^+$ IgD$^-$ memory B cells showed no significant difference across groups. Mann Whitney U test was conducted for pairwise comparison p values < 0.05 were considered significant.

cells was observed when BTKi grouped patients (median = 0.12 per 10^6 lymphocytes) and treatment naïve (median = 41.8 per 10^6 lymphocytes) patients, that approached significance (p = 0.0238) (Fig. 4B). The naïve B cell population (CD19$^+$ CD20$^+$ CD10$^-$ IgD$^+$) was investigated to determine if there were naïve B cells that could recognise SARS-CoV-2 RBD, revealing a similar trend (median = 0.98 per 10^6 lymphocytes for BTKi grouped and median = 32.9 per 10^6 lymphocytes for treatment naïve, p = 0.024) (Fig. 4C). There was no or very little differences in the proportion of RBD$^+$ B cells (CD19$^+$ CD20$^+$ CD10$^-$ CD27$^+$ IgD$^+$) (see Fig. 4D). To determine SARS-CoV-2-specific memory B cells, the analysis was conducted for RBD$^+$ B cells, these cells were gated to select for IgD$^-$ IgG$^+$ B cells. Similarly, there was a significant difference in CD19$^+$ CD20$^+$ CD10$^-$ C27$^+$ IgD$^-$ memory B cells in BTKi treated patients (median = 0 per 10^6 lymphocytes) compared to treatment naïve patients (median = 38.8 per 10^6 lymphocytes, p = 0.011), demonstrating a BTKi treatment effect (Fig. 4E). Spearman's correlation indicated good correlation (> 0.4) of RBD specific memory B cells against early clade variant (0.50), delta (0.58) and omicron variant (0.41) respectively. No difference in antibody secreting cells (ASCs) was observed between the groups (data not shown).

Expansion of CD8$^+$ T cells with distinct phenotype in WM participants after BTKi treatment interruption

We conducted single-cell RNA sequencing on 18,600 (live CD3$^+$ and CD20$^+$ pooled) cells at D3 from treatment naïve, BTKi treated and BTKi paused patient groups (N = 4 each group). Dimensionality reduction using uniform manifold approximation and projection (UMAP) revealed two major clusters of CD4$^+$ and CD8$^+$ T cells and a smaller B cell cluster (Fig. 5A-C). The CD4$^+$ T cell cluster was divided into 6 different sub-clusters (CD4$^+$ T1-T6) and the CD8$^+$ T cell cluster was divided into 3 clusters (CD8$^+$ T1-T3). The dominant T cell clusters were CD4$^+$ T1, T2, T3 (memory) and CD8$^+$ T1 (Fig. 5A-C).

We then examined the percentages of the T cell subsets across the three patient groups. When comparing BTKi treated patients with treatment naïve patients, there was a notable increase in NK-like cytotoxic CD8$^+$ T1 (25% vs. 17%), as well as memory CD4$^+$ T3 T cell subsets (20% vs. 11%), alongside a reduction in CD4$^+$ T1 (32% vs. 45%) and T2 subsets (10% vs. 17%) (see Fig. 5D). Interestingly, there was a further expansion of NK like cytotoxic CD8$^+$ T1 cells (25–48%), and a decrease in CD4$^+$ T1 (17% vs. 20%) and T3 (27 vs. 17%) once BTKi treatment was paused compared to patients treated with continuous BTKi (Fig. 5D) suggesting the treatment interruption had an impact on not only CD8$^+$ but also CD4$^+$ T cell subsets. Statistical analysis using two-proportion Z-test revealed that there was a significant difference only in proportion of CD8$^+$ T1 cells between BTKi treated and BTKi paused groups (p < 1.2e-14) and no other T cell subsets.
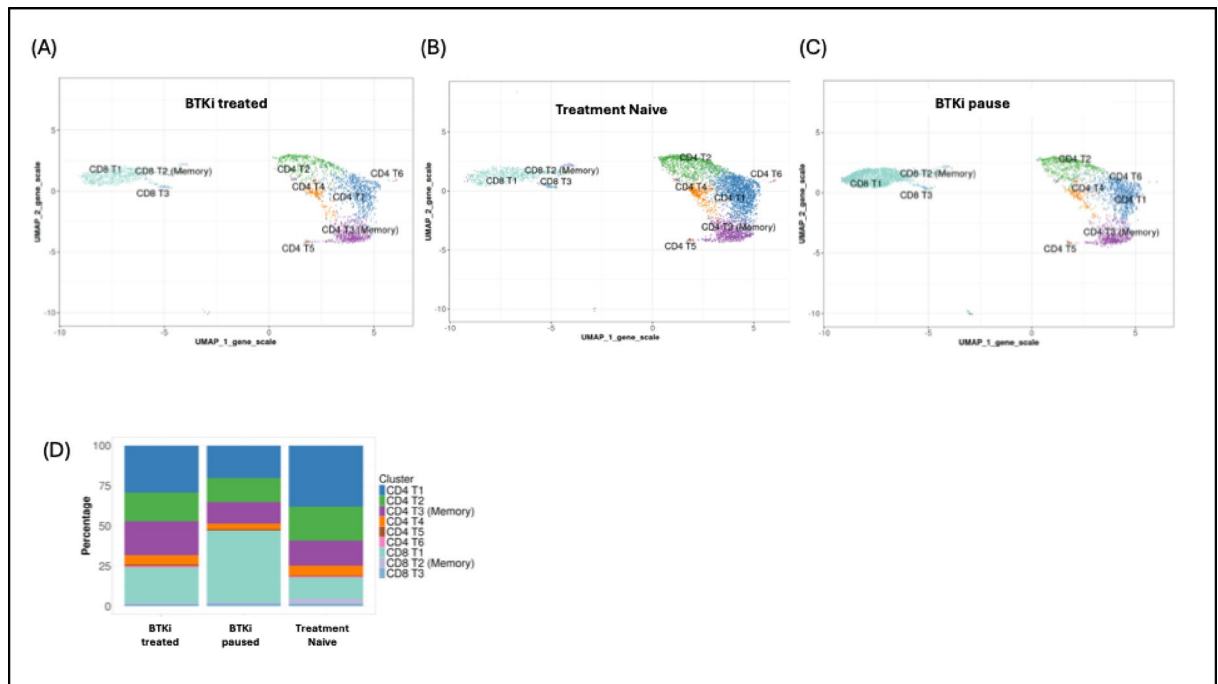
Fig. 5. Dimensionality reduction using UMAP method of single cell RNA sequenced data which includes participants following dose 3 (D3) of mRNA COVID-19 vaccination in BTKi treated, treatment naïve and BTKi paused patients. (**A**) UMAP of BTKi treated patients with increased CD8+ T1 subset of T cells; (**B**) UMAP of treatment naïve patients with subset of T cells with low CD8+ T1 subset and high CD4+ T1 subset of T cells; (**C**) UMAP of BTKi paused patients with higher CD8+ T1 subset of T cells compared to BTKi treated and treatment naïve patients. (**D**) Bar plot of T cell cluster percentages in each patient group.

Initial annotation was conducted using the AbSeq 30 immune marker panel. There was no difference in the protein expression across the treatment groups, therefore the panel was divided according to each cell cluster (Fig. 6). The CD8+ T1 cluster expressed CD45+, CD56+ and CD16+. Both CD4+ T1 and CD4+ T3 clusters exhibited naive T cell phenotype, expressing CD45RA, CCR7+, CD62L+ and CD27+.

We then examined the differential gene expression of these T cell populations within each patient group (Fig. 7A-B). Our analysis revealed that compared to treatment naïve, BTKi treated patients displayed CD8+ T1 subsets with cytotoxic NK-like (CD56+, NCR-1, KLRC2, KLRF1, GNZMB, CCL4) phenotype and genes relevant to T cell development (DGKK, TRDJ1, TYROBP, TRBV6) (Fig. 7A). Notably, BTKi paused patients displayed NK-like cytotoxic and activation genes (KLRF1, NKG7, FcGR3A or CD16, IRF5, ITGAM or CD11b, FASLG) (Fig. 7B)[26]. In contrast, treatment naïve patients exhibited a distinct phenotype with genes such as CXCR5, Granzyme K and CTLA4 as well as IL-7R that regulates T cell survival (see Fig. 7A). Other dominant clusters, CD4+ T1 (CCR7, TNFAIP3, IL6ST) and CD4+ T3 (CCR7, CD127, IL-7R, TCF-7, and CD27) displayed naïve phenotype (see Supplementary Table 3) consistent with the cell surface protein (AbSeq) profile.

Gene set enrichment analysis was performed to determine the canonical immune signalling pathways in the expanded NK like cytotoxic CD8+ T1 cell population (see Fig. 8). Immune pathways such as Fc gamma receptor pathway linked to antigen recognition and PD-L1 (programmed cell death-1) checkpoint inhibitor pathway, was elevated in BTKi treated patients compared to treatment naïve patients (see Fig. 8). Moreover, SLRP (small leucine rich proteoglycans) and MAPK pathway was upregulated in BTKi when compared to BTKi paused patients. In these BTKi paused patient's other pathways were upregulated that were linked to T cell development, differentiation and prolonged T cell survival, namely, GABA, hedgehog and WNT agonist signalling pathways, (see Fig. 8).

Discussion

BTKi are useful therapies for the management of B cell malignancies owing to their high efficacy and favourable tolerability. However, the full extent of the effects of prolonged use of BTKi therapy on the immune system remains unclear. Nevertheless, studies in CLL have shown that alterations induced by BTKi can lead to off-target effects on kinases other than BTK, resulting in dysfunction in the immune response to infections and compromising vaccine effectiveness[27,28]. During the COVID-19 pandemic, work by our group and others demonstrated a reduced seroconversion post 2nd and 3rd dose of the mRNA COVID-19 vaccine in people with WM on long term continuous BTKi therapy. Clinically monitored BTKi interruption strategies have been previously implemented for managing BTKi associated toxicities and symptoms and also vaccine responses[28]. Our group has previously shown that clinically monitored BTKi treatment pause for 3–4 weeks in patients with WM post 2nd and before 3rd dose of the COVID-19 mRNA vaccine lead to seroconversion in majority of these
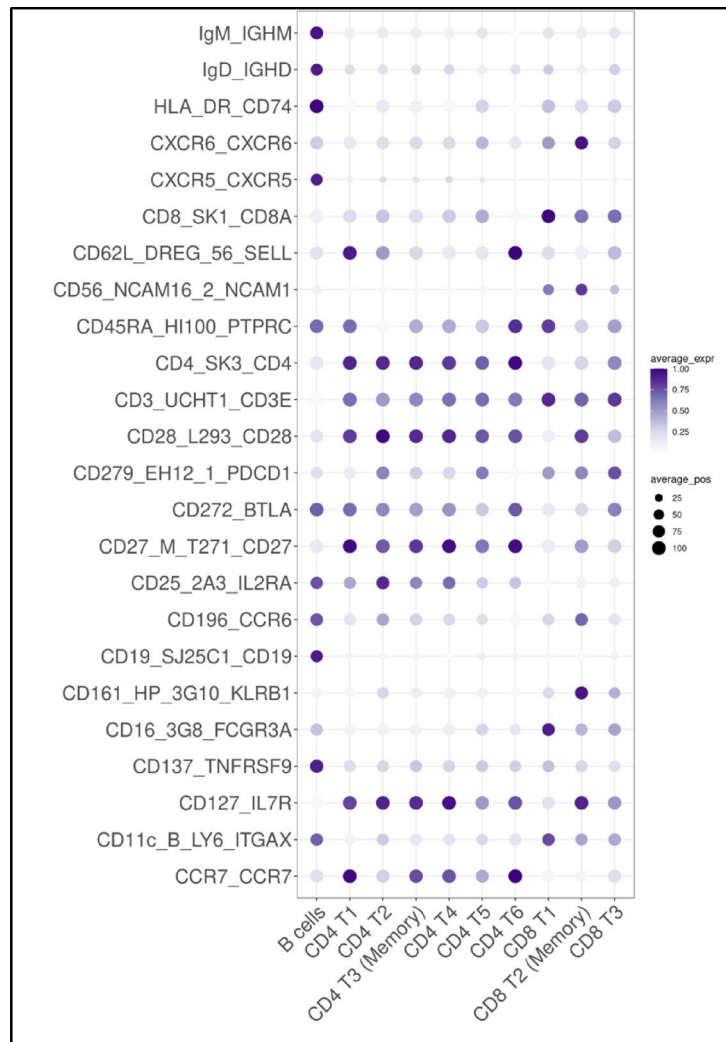
Fig. 6. AbSeq panel of gene markers to annotate all the CD8+ and CD4+ T cell clusters and the B cell clusters. No difference in gene expression was observed between the treatment groups.

patients[13,29]. Hence it was valuable to explore the impact of BTKi treatment interruption in not only CLL but also other B cell malignancies such as WM. Therefore, we interrogated the off-target effects of continuous and interrupted BTKi in WM patients, resulting in novel insights.

Prior immune profiling studies have identified alterations in both innate and adaptive immune compartments, including skewing of T cell subsets, aberrant natural killer (NK) cell function, and dysregulated cytokine profiles. For example, increased cytotoxic CD8+ T cell populations have been reported in WM patients independent of BTKi therapy[30–32], suggesting that the observed expansions may be driven by the disease rather than treatment effects. Nevertheless, our data demonstrates WM disease is associated with an expansion of NK-like CD8+ T cells that is further augmented by BTKi exposure and subsequent treatment interruption, indicating possible off-target immune modulation by these inhibitors.

Comparative studies have also revealed distinct immune signatures correlating with disease stage and treatment response, underscoring the complex interplay between malignant cells and the host immune system[32]. In our study we found that the ratios of CD4+:CD8+ T cells in WM patients, receiving BTKi treatment, had a significantly lower proportion than those observed in healthy controls following three doses of the mRNA COVID-19 vaccination, implying alteration in the immune profile in patients on this immunotherapy. Moreover, patients undergoing BTKi treatment displayed significantly higher levels of CD8+ T cells compared to both treatment-naïve and healthy controls. This increased proportion of CD8+ T cells, is similar to findings in CLL patients undergoing BTKi therapy, a parameter that has been associated with disease progression[33]. We identified a higher proportion of phenotypically exhausted and terminally differentiated T cells in the BTKi treated patients compared to treatment-naïve or healthy controls, aligning with previous observations in CLL studies[34]. However, even with the expansion of CD8+ T cells, we found that that there was no significant increase in proliferative or antigen-specific functionality of these CD8+ T cells. Notably, BTKi treated patients exhibited enhanced CD8+ memory T cell response to Omicron in BTKi-treated patients, but not to the ancestral strain or in CD4+ T cells, suggests a selective effect. BTKi may preferentially support cytotoxic T cell responses, possibly
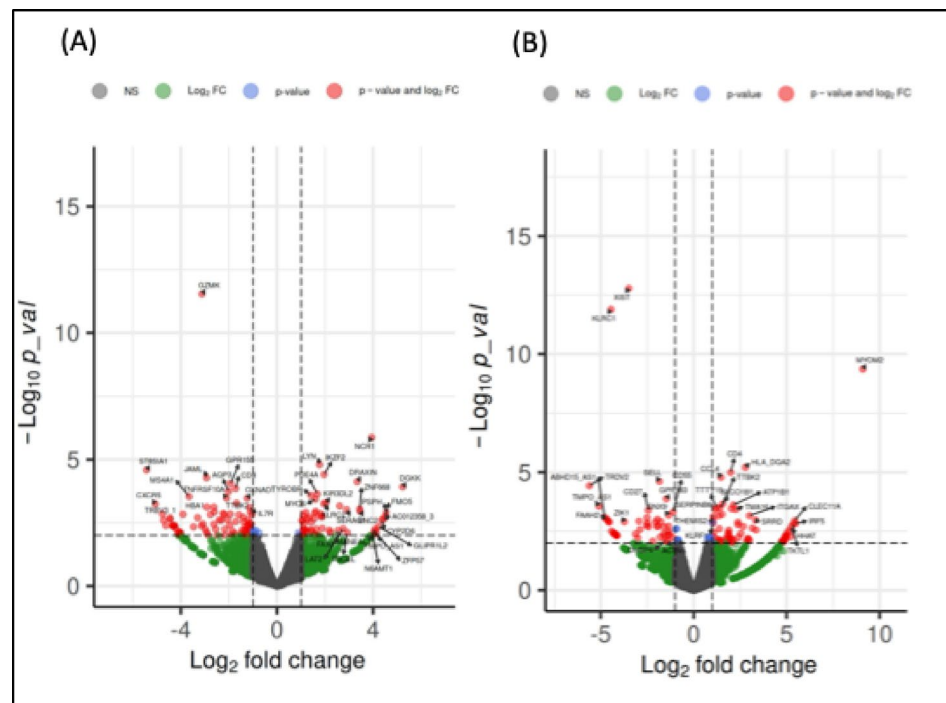
Fig. 7. Differential gene expression of CD8^{+} T1 clusters across BTKi treated, treatment naïve and BTKi pause patients (**A**) Volcano plot with upregulation of genes linked to cytotoxicity and NK like phenotype in CD8^{+} T1 cluster in BTKi treated patients compared to treatment naive. (**B**) Volcano plot of genes associated with cytotoxicity and proliferation in CD8^{+} T1 cluster in BTKi paused patients compared to BTKi continuous treatment.
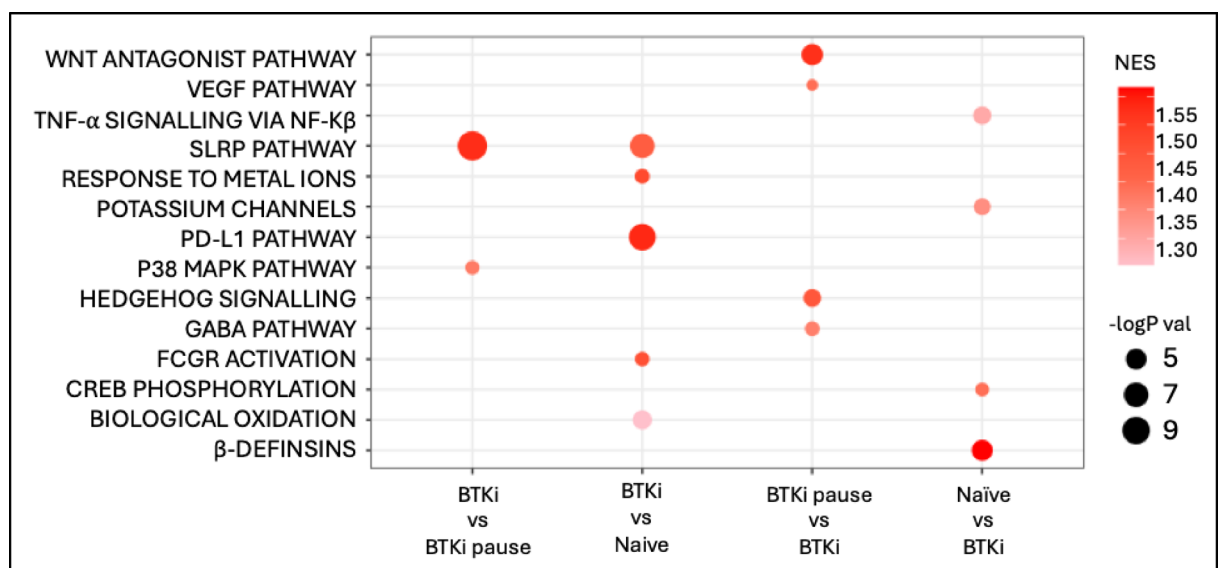

Fig. 8. Pairwise gene set enrichment analysis of CD8^{+} T1 clusters across BTKi treated, treatment naïve and BTKi paused patients. Upregulation of MAPK pathway associated with TCR stimulation and PD-L1 pathway linked to T cell exhaustion observed in BTKi treated compared to treatment naïve. Hedgehog and WNT agonist pathway linked to prolonged T cell survival and proliferation observed in BTKi paused patients compared to continuous BTKi treated patients.

through modulation of innate immunity and antigen presentation. The lack of response to the ancestral strain could reflect waning immunity or antigenic divergence. Overall, these findings highlight differential effects of BTKi on T cell subsets where BTKi treatment shifts the T cell landscape by increasing CD8$^+$ T cell proportions without broad enhancements of their proliferative or antigen specific functions, aside from selective memory response to Omicron strain.

For the first time, we investigated the effects of a BTKi treatment interruption in antigen-specific T cell responses in WM patients. However, the pause did not result in an increase of antigen-specific CD4$^+$ or CD8$^+$ T cells as compared to continuous BTKi treatment, indicating the expanded proportion of CD8$^+$ T cells was not associated with superior pathogen-specific response, possibly due to the terminally differentiated/exhausted phenotype.

We then examined the grouped BTKI (treated and paused) patients as we did not find significant different with pausing the treatment, potentially due to a short duration of interruption for 2–3 weeks. Notably, in the grouped BTKi (treated and paused) patients the antigen specific or RBD specific memory B cells decreased compared to continuous treatment and these patients had high neutralising antibody titres in serum. This likely reflects impaired B cell survival and differentiation under BTKi, leading to fewer circulating memory B cells but preserved plasma cell derived antibody production. Low proportions of RBD-specific memory B cells have been reported in CLL patients on long-term continuous treatment post booster mRNA COVID-19 vaccination[35]. Strategies to modulate the interruption periods under clinical monitoring or the requirement of combination treatment strategies could potentially help augment these responses.

Transcriptomic analysis revealed that pausing the BTKi treatment in patients triggered an expansion of already prevalent NK-like cytotoxic memory CD8$^+$ T cell population. This expansion occurred when BTKi treatment was interrupted for a short duration. Previously, ibrutinib has been associated to negatively impact the NK-like CD8$^+$ T cell function characterized by reduction in T cell proliferation and activation leading to CD8$^+$ T cell impairment[36]. Moreover, BTKi treatment also impacted on the transcriptome of CD4$^+$ T cell subsets. We found that naïve CD4$^+$ T cell population was higher in BTKi treated patients compared to treatment naïve patients, therefore this therapy could play a role in altering the CD4$^+$ T cell compartments.

We further investigated the immune pathways that were upregulated after BTKi treatment patients compared to no treatment patients and we found that in the CD8$^+$ T cells, there was upregulation of immune pathways that include immune checkpoint PD-L1 pathway, that plays a role in maintaining immune homeostasis and regulates T cell proliferation during an inflammatory response and Fc gamma receptor pathway involved in improving antigen recognition[37]. Cellular pathways that were upregulated included SLRP (small leucine-rich proteoglycans) was upregulated in these patients, modulates inflammation and cellular repair[38]. Moreover, altered metal ion pathways linked to cellular metabolism and function in BTKi treated patients indicated a cellular stress response induced by the treatment regimen. In contrast, BTKi interrupted patients displayed an upregulation of the GABA pathway associated with proliferation and cytokine production. Hedgehog signalling linked to T cell activation, differentiation and cytoxicity was additionally found to be upregulated in these patients[4].

Our study has several limitations. First, we acknowledge the small sample size and there may be heterogeneity across the participant population. Second, the BTKi treatment pause was patient initiated and there was minor variation in the pause duration. Third, we did not further study the BTKi treatment pause participants after they resumed their BTKi treatment. Fourth, genomic analysis and mutational status of these participants was unavailable as it is currently not the standard of care for management of WM in Australia.

BTKi remain an important tool for the management of several B cell malignancies. However, it is important to recognise their detrimental effect on seroconversion to vaccines. Strategies around how best to counter this is an area of ongoing interest, particularly considering the ongoing COVID-19 pandemic. What is less recognised is the off-target effect of these agents on other lymphocyte subsets. This work demonstrates a strong association of BTKi with NK-like memory cytotoxic CD8$^+$ T-cells with an exhausted phenotype, with additional changes in the CD4$^+$ subsets. The NK-like memory cytotoxic CD8$^+$ T cell population increases in proportion following a BTKi treatment interruption. These changes appear to be a direct result of this specific therapy and have not been reported in XLA.

In summary, our study demonstrates that BTKi therapy in WM patients is associated with a distinct reshaping of the T cell compartment, most notably the expansion of cytotoxic NK-like CD8$^+$ T cells with a unique transcriptional signature. This off-target effect persists following treatment interruption. Despite impaired B cell responses, T cell immunity to SARS-CoV-2, particularly CD8$^+$ responses to the omicron variant remains detectable, underscoring a degree of preserved cellular immunity. Our findings complement provides novel insights into the impact of the disease and the BTKi therapy on immune effector populations. These findings have important implications for understanding the broader immunological impact of BTKi, informing vaccine strategies, and guiding immune monitoring in patients receiving targeted therapies. However, discrepancies between studies may stem from differences in patient cohorts, treatment regimens, or profiling methodologies. Larger, longitudinal studies that conduct transcriptomic analysis at the protein level and function level will be essential to clarify the clinical implications of these immune alterations and their potential as biomarkers of treatment response or toxicity. In addition, further studies on the impact of varying BTKi treatment interruption on immune function and vaccine efficacy are warranted.

Data availability

The datasets generated and/or analysed during the current study are available in the SRA NCBI repository, [https://www.ncbi.nlm.nih.gov/sra/PRJNA1228938 AND ACCESSION NUMBER: PRJNA1228938]. For any further information or requests regarding the data, please contact the corresponding author, Dr Priyanka Hastak (priyanka.hastak@unsw.edu.au).

References

1. Ntanasis-Stathopoulos, I. et al. Current and novel BTK inhibitors in waldenström's macroglobulinemia. *Ther. Adv. Hematol.* **12**, 2040620721989586 (2021).
2. Burger, J. A. Bruton tyrosine kinase inhibitors: present and future. *Cancer J.* **25** (6), 386–393 (2019).
3. Wang, H. et al. Bruton tyrosine kinase inhibitors in B-cell lymphoma: beyond the antitumour effect. *Experimental Hematol. Oncol.* **11** (1), 60 (2022).
4. Alu, A. et al. BTK inhibitors in the treatment of hematological malignancies and inflammatory diseases: Mechanisms and clinical studies. *J. Hematol. Oncol.* **15** (1), 138 (2022).
5. Wu, J. et al. Second-generation inhibitors of Bruton tyrosine kinase. *J. Hematol. Oncol.* **9** (1), 80 (2016).
6. Cheah, C. Y. et al. A phase 1 study with the novel B-cell lymphoma 2 (Bcl-2) inhibitor Bgb-11417 as monotherapy or in combination with zanubrutinib (ZANU) in patients (Pts) with CLL/SLL: preliminary data. *Blood* **140** (Supplement 1), 2321–2323 (2022).
7. Mhibik, M., Wiestner, A. & Sun, C. *Harnessing the effects of BTKi on T cells for effective immunotherapy against CLL. Int. J. Mol. Sci.*, **21**(1). (2019).
8. Yin, Q. et al. Ibrutinib therapy increases T cell repertoire diversity in patients with chronic lymphocytic leukemia. *J. Immunol.* **198** (4), 1740–1747 (2017).
9. Puzzolo, M. C. et al. TH2/TH1 shift under ibrutinib treatment in chronic lymphocytic leukemia. *Front. Oncol.* **11**, 637186 (2021).
10. Beaton, B. et al. Patients with treated indolent lymphomas immunized with BNT162b2 have reduced anti-spike neutralizing IgG to SARS-CoV-2 variants, but preserved antigen-specific T cell responses. *Am. J. Hematol.* **98** (1), 131–139 (2023).
11. Haggenburg, S. et al. Quantitative analysis of mRNA-1273 COVID-19 vaccination response in immunocompromised adult hematology patients. *Blood Adv.* **6** (5), 1537–1546 (2022).
12. Gavriatopoulou, M. et al. Poor neutralizing antibody responses in 106 patients with WM after vaccination against SARS-CoV-2: A prospective study. *Blood Adv.* **5** (21), 4398–4405 (2021).
13. Rankin, K. et al. Immune response to COVID-19 vaccination in patients with Waldenström macroglobulinaemia who pause their BTKi therapy. *eJHaem* **4** (3), 728–732 (2023).
14. Saberi, D. et al. Bruton's tyrosine kinase as a promising therapeutic target for multiple sclerosis. *Expert Opin. Ther. Targets.* **27** (4–5), 347–359 (2023).
15. Zaunders, J. J. et al. High levels of human antigen-specific CD4 + T cells in peripheral blood revealed by stimulated coexpression of CD25 and CD134 (OX40). *J. Immunol.* **183** (4), 2827–2836 (2009).
16. Phetsouphanh, C. et al. *High titre neutralizing antibodies in response to SARS–CoV–2 infection require RBD–specific CD4 T cells that include proliferative memory cells. Front. Immunol.*, 13. (2022).
17. Zaunders, J. et al. Mapping the extent of heterogeneity of human CCR5 + CD4 + T cells in peripheral blood and lymph nodes. *AIDS* **34** (6), 833–848 (2020).
18. Zaunders, J. et al. Possible clearance of transfusion-acquired nef/LTR-deleted attenuated HIV-1 infection by an elite controller with CCR5 Δ32 heterozygous and HLA-B57 genotype. *J. Virus Eradication.* **5** (2), 73–83 (2019).
19. Abayasingam, A. et al. Long-term persistence of RBD(+) memory B cells encoding neutralizing antibodies in SARS-CoV-2 infection. *Cell. Rep. Med.* **2** (4), 100228 (2021).
20. Ulbrich, J., Lopez-Salmeron, V. & Gerrard, I. BD rhapsody™ Single-Cell analysis system workflow: From sample to multimodal Single-Cell sequencing data. *Methods Mol. Biol.* **2584**, 29–56 (2023).
21. Lun, L., Bach, A. T. K. & Marioni, J. C. Pooling across cells to normalize single-cell RNA sequencing data with many zero counts. *Genome Biol.* **17** (1), 75 (2016).
22. Stuart, T. et al. Comprehensive integration of Single-Cell data. *Cell* **177** (7), 1888 (2019). –1902.e21.
23. Squair, J. W. et al. Confronting false discoveries in single-cell differential expression. *Nat. Commun.* **12** (1), 5692 (2021).
24. Liberzon, A. et al. The molecular signatures database (MSigDB) hallmark gene set collection. *Cell. Syst.* **1** (6), 417–425 (2015).
25. Korotkevich, G. et al. *Fast gene set enrichment analysis.* bioRxiv, : p. 060012. (2021).
26. Pizzolato, G. et al. Single-cell RNA sequencing unveils the shared and the distinct cytotoxic hallmarks of human TCRVδ1 and TCRVδ2 γδ T lymphocytes. *Proc. Natl. Acad. Sci. U S A.* **116** (24), 11906–11915 (2019).
27. Pleyer, C. et al. BTK inhibitors impair humoral and cellular responses to Recombinant Zoster vaccine in CLL. *Blood Adv.* **6** (6), 1732–1740 (2022).
28. Bryer, E. et al. Booster and Btki interruption improve response to Sars-Cov-2 vaccine in patients with CLL. *Blood* **140** (Supplement 1), 9896–9897 (2022).
29. Barber, V. S. et al. Protocol for a multicentre randomised controlled trial examining the effects of temporarily pausing Bruton tyrosine kinase inhibitor therapy to coincide with SARS-CoV-2 vaccination and its impact on immune responses in patients with chronic lymphocytic leukaemia. *BMJ Open.* **13** (9), e077946 (2023).
30. Mhibik, M., Wiestner, A. & Sun, C. Harnessing the effects of BTKi on T cells for effective immunotherapy against CLL. *Int. J. Mol. Sci.* **21** (1), 68 (2020).
31. Sklavenitis-Pistofidis, R. et al. Targeting Bruton tyrosine kinase: A novel strategy in the treatment of B-cell lymphomas. *Forum Clin. Oncol.* **8** (1), 7–14 (2017).
32. Li, L. et al. Ibrutinib directly reduces CD8 + T cell exhaustion independent of BTK. *Front. Immunol.* **14**, 1201415 (2023).
33. Nunes, C. et al. Expansion of a CD8 + PD-1 + Replicative senescence phenotype in early stage CLL patients is associated with inverted CD4:CD8 ratios and disease progression. *Clin. Cancer Res.* **18** (3), 678–687 (2012).
34. Liu, Y., Song, Y. & Yin, Q. Effects of ibrutinib on T-cell immunity in patients with chronic lymphocytic leukemia. *Front. Immunol.* **13**, 962552 (2022).
35. Lyski, Z. L. et al. Cellular and humoral immune response to mRNA COVID-19 vaccination in subjects with chronic lymphocytic leukemia. *Blood Adv.* **6** (4), 1207–1211 (2022).
36. Davis, J. E. et al. Ibrutinib protects T cells in patients with CLL from proliferation-induced senescence. *J. Transl Med.* **19** (1), 473 (2021).
37. Boussiotis, V. A., Chatterjee, P. & Li, L. Biochemical signaling of PD-1 on T cells and its functional implications. *Cancer J.* **20** (4), 265–271 (2014).
38. Park, J. E. et al. Leukocyte-associated immunoglobulin-like receptor 1 inhibits T-cell signaling by decreasing protein phosphorylation in the T-cell signaling pathway. *J. Biol. Chem.* **295** (8), 2239–2247 (2020).

Acknowledgements

Author contributions

P.H and S.C.S wrote the main manuscript text together. C.P provided feedback on manuscript, wrote part of the result section, generated figures. Z.Z, R.A.B, E. K and L.B.S wrote part of the result section and generated figures. All authors reviewed and provided detailed feedback on the final version of the manuscript.

Declarations

Competing interests

The authors declare no competing interests.

Additional information

Supplementary Information The online version contains supplementary material available at https://doi.org/1 0.1038/s41598-025-18450-8.

Correspondence and requests for materials should be addressed to P.H.

Reprints and permissions information is available at www.nature.com/reprints.

Publisher's note Springer Nature remains neutral with regard to jurisdictional claims in published maps and institutional affiliations.